Control Set Reduction for PMSM Predictive Controller via Assisted Learning Algorithm

Michal Kozubik
CEITEC - Central European Institute of Technology
Brno University of Technology
Brno, Czech Republic
Michal.Kozubik@ceitec.vutbr.cz

Pavel Vaclavek
CEITEC - Central European Institute of Technology
Brno University of Technology
Brno, Czech Republic
Pavel.Vaclavek@ceitec.vutbr.cz

***Abstract*—This paper introduces innovative methods for reducing the control set in finite control set model predictive control of the Permanent Magnet Synchronous Motor powered by a 3-level voltage source inverter. The primary objective of this reduction is to address a crucial factor in the computational burden of the control algorithm—the exponential growth in the number of potential switching state combinations forming the controller's control set with an increasing prediction horizon length. The proposed methods aim to decrease the number of switching states necessary for evaluation, mitigating the aforementioned exponential growth. These methods leverage information about the controller's behavior. The first method relies solely on the count of transitions between individual switching states. Additionally, the second method incorporates information about the states of the controlled motor to construct a decision tree, forming the new control set. The behavior of the controllers with reduced and complete control sets is compared in the simulation experiment, emphasizing the proper tracking of the requested angular speed and their overall computational complexity.**

***Index Terms*—finite control set, model predictive control, nonlinear control, permanent magnet synchronous motor, supervised learning**

I. Introduction

The advantages of permanent magnet synchronous motors (PMSMs), such as the power-to-scale ratio and high reliability [1], make them available for wide use in many industrial applications. However, their properties, such as a combination of a short electrical time constant and, in comparison, a longer mechanical time constant, cause difficulties in the controller design. The cascade controller scheme can solve this problem. On the other hand, this structure has issues dealing with the constraints of different motor states, e.g., stator currents. Thus, researchers aim at the utilization of various novel control methods.

Nonlinear model predictive control (NMPC) belongs to the group of these researched methods. [2], [3] Its multi-variable and multi-constraint nature makes it stand out among advanced control algorithms. However, its computational complexity, mixed with the short sampling times necessary for proper motor control, poses a challenge from an implementation point of view.

Utilizing the full potential of NMPC in its multi-variability requires a longer prediction horizon, which further increases its computational complexity. For this reason, most researchers focus on the control of only one variable. The most prevalent is the Predictive Current Control [4]–[6] followed by Predictive Torque Control (PTC) [7], [8] and Predictive Speed Control (PSC) [9]. In [10], [11], authors successfully implemented the controller to control both speed and current. However, the computational complexity of multi-step predictive control still causes implementational problems [12].

This paper aims to decrease the computational complexity of the NMPC controller providing control of both the speed and the current of PMSM fed by the 3-level Voltage Source Inverter (VSI). For this purpose, the paper proposes two methods of control set reduction. These methods build upon the data about the transitions between individual switching states of VSI. The first method selects the desired number of most prevalent transitions and forms to control set out of them. The second one uses the data about transition and measurement to learn a decision tree, forming the reduced control set.

The organization of the paper is following. Section II introduces the control scheme for the nonlinear model predictive speed control of PMSM. The problem of the computational burden and its dependency on the length of the prediction horizon is outlined. The following section presents the experiment that served for the analysis of the transfers between individual switching states. Section IV presents the methods for reducing the control set based on the data acquired in a previous section. The following section compares the overall performance and computational time demands of controllers working with the reduced control and the controller with the complete control set in the simulation experiment. The last section concludes this paper.

II. Problem Definition

The Finite Control Set Nonlinear Model Predictive Speed Control aims to find the optimal switching state $s(k)$ of the Voltage Source Inverter that guarantees the minimal value of a given cost function. This cost function usually covers the minimization of the tracking error between the requested value of angular speed $\omega_{m,r}$ and its actual value ω_m and penalization of the values of current and the transfers between switching states. [13], [14]

Figure 1 shows the control scheme of such a predictive con-

troller. After measurement of necessary states - phase currents i_{abc}, angular speed ω_m and mechanical angular position ϑ_m, currents are transformed to dq-reference frame. Then the model

$$\begin{aligned} i_{d|k+1} &= i_{d|k} + (T_s/L_d)\left(-R_s i_{d|k} + P_p L_q i_{q|k}\omega_{m|k} + u_{d|k}\right) \\ i_{q|k+1} &= i_{q|k} + (T_s/L_q)\left(-R_s i_{q|k} - P_p L_d i_{d|k}\omega_{m|k}\right) + \\ &\quad + (T_s/L_q)\left(-Pp\Psi_{PM}\omega_{m|k} + u_{q|k}\right) \\ \omega_{m|k+1} &= \omega_{m|k} + (T_s/J)[(3P_p/2)\left(\Psi_{PM} i_{q|k} + \right. \\ &\quad \left. + (L_d - L_q)\, i_{d|k} i_{q|k}\right)] \\ \vartheta_{m|k+1} &= \vartheta_{m|k} + T_s\omega_{m|k}, \end{aligned} \tag{1}$$

where R_s is the stator winding resistance, $L_{d,q}$ are the rotor inductance components, P_p is the number of pole pairs, Ψ_{PM} is the permanent magnet flux, J is the moment of inertia, T_s is the smapling period and k represents the discrete unit of time; is evaluted for given input voltage vector $\mathbf{u} = \{u_{d|k}\ u_{q|k}\}$.
With this model, the controller solves the optimization problem

$$s(k) = \underset{J}{\operatorname{argmin}}\{C_J(k) \mid 0 \leq J < |S|\}, \tag{2}$$

where S is the Control Set of possible switching states, C_J represents the cost function value for J-th member of the control set. Each member of the set S is a vector, which consists of switching states that should be applied in individual sampling times - generating the aforementioned voltage vector. The standard approach in obtaining the cost function value is to evaluate all possible switching state combinations across the prediction horizon length N [15]. The number of possible combinations grows exponentially, where the base of the exponential function is the number of switching states for a given voltage source inverter. This paper deals with the 3-level VSI; therefore, 27 possible switching states exist. Table I displays their overview.
For the given number of possible switching states and the length of the prediction horizon, index J contains the information about the candidate vector $\mathbf{v}_J$. In the presented case of 27 possible switching states

$$\mathbf{v}_J = \begin{bmatrix} \mathrm{mod}(J, 27) & \cdots & \mathrm{mod}(\lfloor J/27^{N-1} \rfloor, 27) \end{bmatrix}, \tag{3}$$

where $\lfloor\rfloor$ denotes the floor (round down) function and $\mathrm{mod}(a, b)$ is modulo function defined as $\mathrm{mod}(a, b) = a - b(\lfloor a/b \rfloor)$.
The exponential growth in the number of combinations leads to the problem with the ability of the controller to find the optimal switching state in the time necessary for proper motor control, even on platforms performing parallel computing such as FPGAs and GPUs.

III. Switching State Transfer Analysis

This section deals with the design of the experiment, which results served as a basis for the design of the reduced control set.

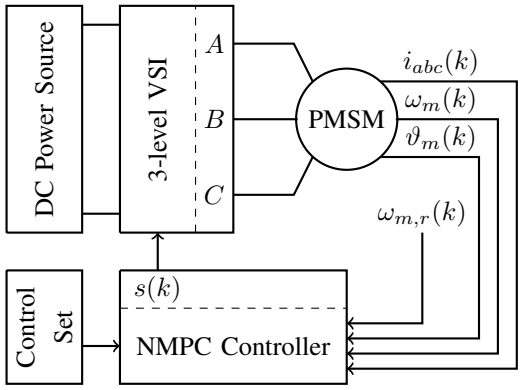

Fig. 1: Control Scheme

TABLE I: Switching State Overview

$s(k)$	A	B	C
0	0	0	0
1	0	0	0.5
2	0	0	1
3	0	0.5	0
4	0	0.5	0.5
5	0	0.5	1
6	0	1	0
7	0	1	0.5
8	0	1	1
9	0.5	0	0
10	0.5	0	0.5
11	0.5	0	1
12	0.5	0.5	0
13	0.5	0.5	0.5
14	0.5	0.5	1
15	0.5	1	0
16	0.5	1	0.5
17	0.5	1	1
18	1	0	0
19	1	0	0.5
20	1	0	1
21	1	0.5	0
22	1	0.5	0.5
23	1	0.5	1
24	1	1	0
25	1	1	0.5
26	1	1	1

A. Data Acquisition

Gathering data for the control set reduction consisted of two steps. The first step was the design of the FCS-Controller working with the whole control set. The following step was the data acquisition itself.
First, the control algorithm was implemented on the platform Jetson Xavier utilizing the parallelism of evaluating each candidate solution vector in its specific thread.
The controller design took into account the standard re-

TABLE II: Parameters of PMSM

Parameter	Value	Unit
R	0.38	Ω
L_d	0.405	mH
L_q	0.665	mH
Ψ_{PM}	0.02594	Wb
Pp	3	–
J	$446 \cdot 10^{-6}$	$\mathrm{kg\,m^2}$
U_{DC}	12	V
I_R	6	A

TABLE III: Controller parameters

Parameter	Value
w_ω	0.50
w_{i_q}	$0.50 \cdot 10^{-9}$
w_{i_d}	$0.50 \cdot 10^{-8}$
w_{SW}	$0.85 \cdot 10^{-7}$
w_{IC}	$0.25 \cdot 10^{-9}$
N	3
T_s	10 µs

quirements for motor speed control - monitoring the desired value and keeping the stator current within the defined limits. Meeting these requirements was ensured by a cost function in the form of

$$\begin{aligned} C_J(k) = &\sum_{i=1}^{N} \left(w_\omega \left(\omega_{m,r} - \omega_m(k+i)\right)^2 + w_{i_q} i_q^2(k+i) \right) + \\ &+ \sum_{i=1}^{N} \left(w_{i_d} i_d^2(k+i) + w_{\mathrm{SW}} |s(k+i) - s(k+i-1)| \right) + \\ &+ \sum_{i=1}^{N} -w_{\mathrm{IC}} \log\left(I_R^2 - i_d^2(k+i) - i_q^2(k+i) \right), \end{aligned} \tag{4}$$

where w_ω, w_{i_q}, w_{i_d} and w_{SW} are weighting coefficients for the tracking of requested angular speed, direct and quadrature component of the current, and the number of switchings performed. The last term deals with constraint limiting the current vector by its rated value. The coefficient w_{IC} affects the skewness of this barrier function. [16]
Described algorithm constants were tuned for the motor with parameters presented in Table II. The table also contains the rated current I_R value and the power supply voltage U_{DC}. Tuned algorithm parameters are in Table III.

The reference angular speed signal designed to collect transitions between switching states contained a raising ramp with a slope higher than the possible torque achievable by the controlled motor. After reaching the defined value, the request stayed constant. Then the decreasing ramp with a less steep slope, achievable by the motor, followed until the measured angular speed settled on zero. The same waveform,

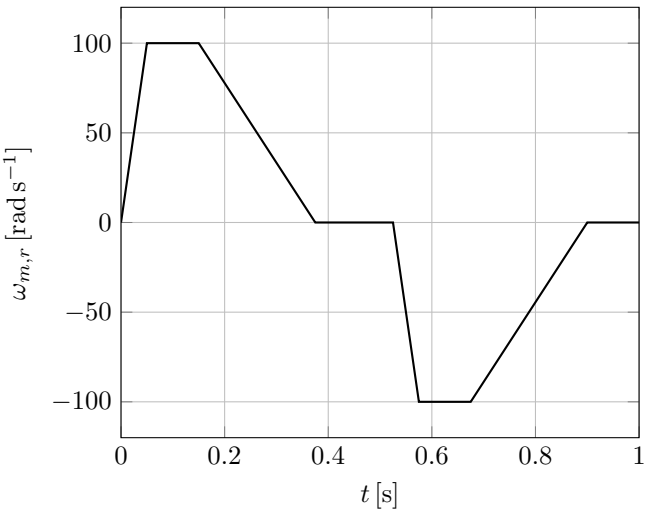

Fig. 2: Requested angular speed for the data acquisition

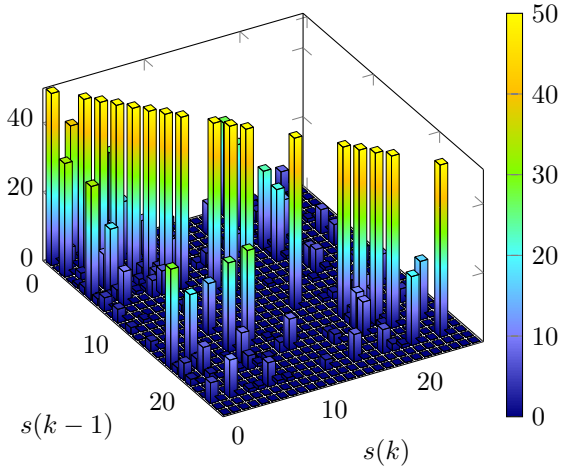

Fig. 3: Transitions between switching states

but for negative angular speeds, followed. Figure 2 shows the complete waveform.
This composition of the reference signal covered the possibilities of demands for both high and low torque for positive and negative angular speed.

B. Data Analysis

The bar chart in Figure 3 shows the transitions between individual switching states. As expected, the most prevalent transitions were not, in fact, transitions but keeping the original switching state. In the figure, these are the peaks on the diagonal whose values had to be saturated for other transitions to be visible.
As the figure shows, many possible state transitions are missing. On top of that, some states did not occur at all. A typical example is the case of states 26 and 13 because, from the model perspective, the generated voltage is the same for these states and the state 0. These results suggest that the evaluation of many of the possible switching state combinations is not necessary for the proper function of the control algorithm.

IV. Proposed Reductions

Previous section has shown on gathered data, that it is not necessary to compute the cost function for all candidate vectors from the original control set. Based on the acquired data, this section presents two methods of control set reduction.

A. Raw Data Based Control Set

The basis of the first method for creating a reduced control set is a simple idea based directly on the measured data presented in Figure 6. During the prediction stage, the algorithm would evaluate only the first n most frequent transitions. This approach can have a problem in the original data acquisition because an incorrectly designed request signal can affect the number of transitions.

On top of that, the choice of parameter n has a significant impact on the controller behavior. For example, setting $n = 4$ allows the controller to switch only one phase; therefore, making it a controller of 2-level VSI with the reduced control set.

B. Decision Tree Based Control Set

A control set reduction based only on transitions does not take advantage of the additional data used for control. The second proposed approach, on the other hand, attempts to utilize this data. For example, one can assume that the applicable combinations for deceleration are different from those for acceleration.

This approach uses the algorithm [17] for decision tree learning to create multiple reduced control sets. Measurement of motor states then specifies which control set would be used in the given control value computation.

The learning algorithm of the decision tree worked with a feature vector constructed as

$$\mathbf{x} = \begin{bmatrix} s(k) & \omega_{m,r}(k) & \omega_m(k) & i_d(k) & i_q(k) & \Delta\omega_m(k) \end{bmatrix}^T,$$

where $\Delta\omega_m(k)$ is the difference between the requested and measured angular speeds. The pattern represented the next switching state. As the data in the figure 3 show, the controller tends to keep the switching state as long as possible. Therefore, this transition was always presumed to be present, and the learning algorithm did not use the data representing it.

Each leaf of the tree denotes the next possible switching state for the conditions the learning algorithm stated. Aggregating these leaves and conditions into groups of $n - 1$ leaves and the original switching state creates the reduced control set for given system states.

This approach covers a broad number of switching state combinations without the need for the control set expansion. Thus, keeping the number of evaluated switching state combinations lower than the Raw Data Based Control Set.

V. Simulation Results

This section compares proposed reduced control set approaches with the controller using the complete control set (cCS). All experiments are performed in PIL simulation, in which Jetson Xavier works as a platform for the execution of the control algorithm of the PMSM simulated in Simscape.

The parameters of PMSM and the cost function are the same as in the data acquisition section (Tabs II and III). The Raw Data Based Control Set (rdCS) worked with the eight possible switching states, leading to 512 possible switching state combinations. The second mentioned - Decision Tree Based Control Set (dtCS) - worked with four possible switching states, thus, 64 possible combinations.

The designed reference signal was composed of ramps connecting the constant values of angular speeds. To differ from the original signal used for the data acquisition, the slope of the ramps and the order of the constant values is different. Furthermore, the final constant value of the requested angular speed was $30\,\mathrm{rad\,s^{-1}}$ to test whether the controller can keep different constant values than the ones used for the construction of reduced control sets.

Figure 4a displays the result of the speed tracking experiment. The shallow comparison says that all controllers achieved similar behavior. A more thorough analysis shows slight differences in the controllers' performance. The controller working with rdCS tends to oscillate more than the dtCS. In time $3.25\,\mathrm{s}$, there was a larger overshoot of the dtCS-controlled motor compared to others. In Table IV are speed mean square errors of all tested controllers in comparison to the requested angular speed ($MSE_{\omega_{m,r}}$) and the cCS-controller (MSE_{cCS}) defined by the relations, expecting starting time of experiment to be zero,

TABLE IV: Speed Mean Square Error Overview

	MSE_{cCS}	$MSE_{\omega_{m,r}}$
cCS	–	4.3726
rdCS	0.0464	4.6046
dtCS	0.2407	5.7777

$$MSE_{\omega_{m,r}} = \frac{T_s}{t_f} \sum_{i=0}^{\frac{t_f}{T_s}-1} \left(\omega_{m,r}(i) - \omega_{m,C}(i)\right)^2 \tag{5}$$

$$MSE_{cCS} = \frac{T_s}{t_f} \sum_{i=0}^{\frac{t_f}{T_s}-1} \left(\omega_{m,cCS}(i) - \omega_{m,C}(i)\right)^2, \tag{6}$$

where t_f is the final time of the experiment and $\omega_{m,C}$ represents the speed achieved by the motor controlled by the given controller.

The attained results indicate dtCS-controller's behavior was more similar to the cCS-controller and outperformed the rdCS-controller.

Currents in Figures 4b, 4c do not evoke similar behavior observed on the speeds. Even with such different current values, all controllers were able to keep the current within a defined limit, as shown in Figure 5. As in the case of speed, the dtCS-controller outperformed the controller with rdCS from the MSE point of view. Calculated mean square errors from the cCS of quadrature current part of 0.0496 for

the dtCS-controller and 0.1024 for rdCS again show that dtCS outperformed the second mentioned. A similar case was the direct part of the current. Especially the notable peaks in the i_d waveform led to a much worse value of MSE.
The most crucial factor of the current waveform was the behavior of both controllers when the requested value of angular speed was zero. The controllers with a reduced control set kept switching between two states, as shown in Figure 6. This switching resulted in the oscillations of the stator current. Compared with the cCS-controller, which turned all phases off, this behavior is unwanted because it leads to unnecessary energy consumption, thus, reducing the efficiency of the motor control.
The final factor of the comparison is the time required to calculate the control value. The following times are averages across fifty measurements. First, the controller working with the complete control set needed on average $650\,\mu s$ to evaluate the optimal switching state. The reason for such high computational demands was the necessity for some sequential computation because of the implementation platform capabilities. The time needed by the rdCS-controller was $45\,\mu s$. Even though the dtCS-controller needed to evaluate only 64 possible combinations, its time demands rose because of the necessity to evaluate the decision tree. Therefore, the dtCS-controller needed $20\,\mu s$ to calculate the switching state.

VI. Conclusion

This paper presented two original methods for reducing the computational complexity of the Finite Control Set Model Predictive Controller controlling the speed and the current of a permanent magnet synchronous motor fed by a 3-level voltage source inverter.
The main idea of the proposed methods is to reduce the number of combinations needed to evaluate for proper computation of the VSI switching state. The data acquired during the experiment served as a basis for the presented methods.
The first method uses information about the transfers between individual states to construct the reduced control set. The second proposed method combines the measurement of the motor's states and the machine learning algorithm to construct the decision tree, which then constructs multiple reduced control sets and decides which one to use and when.
The presented methods were compared with the controller using the complete control set. The comparison has shown that the controller working with the decision tree surpassed the second one in both dynamical behavior and computational demands.
The achieved results created a new approach in implementing FCS-NMPC of PMSM, thus, making it more suitable for the computation in sampling times necessary for the proper motor control. Future research will deal with the application of presented methods to more complex voltage source inverters. Also, further code optimization can allow the real-time control of PMSM using FCS-NMPC.

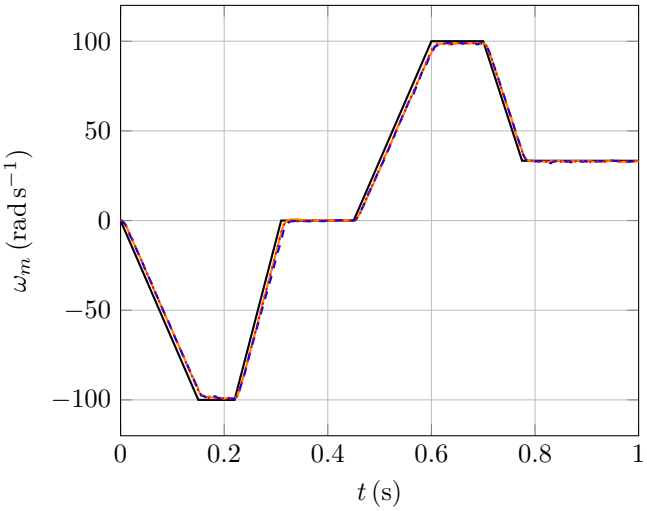

(a) Angular speed during the experiment, black - reference, red - cCS, blue - rdCS, orange - dtCS.

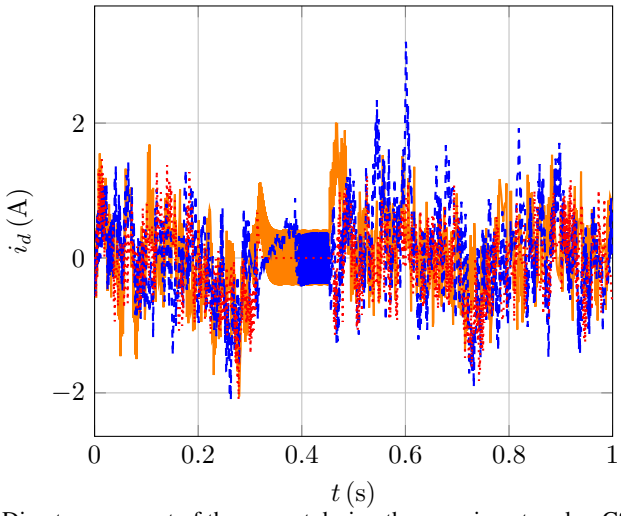

(b) Direct component of the current during the experiment, red - cCS, blue - rdCS, orange - dtCS.

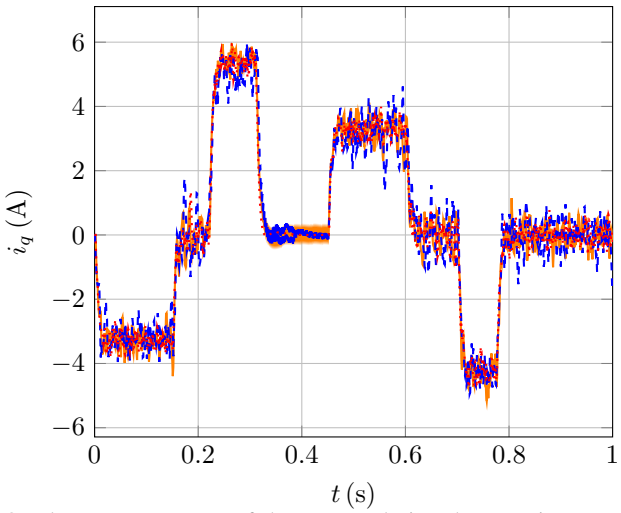

(c) Quadrature component of the current during the experiment, red - cCS, blue - rdCS, orange - dtCS.

Fig. 4: Results of the second experiment.

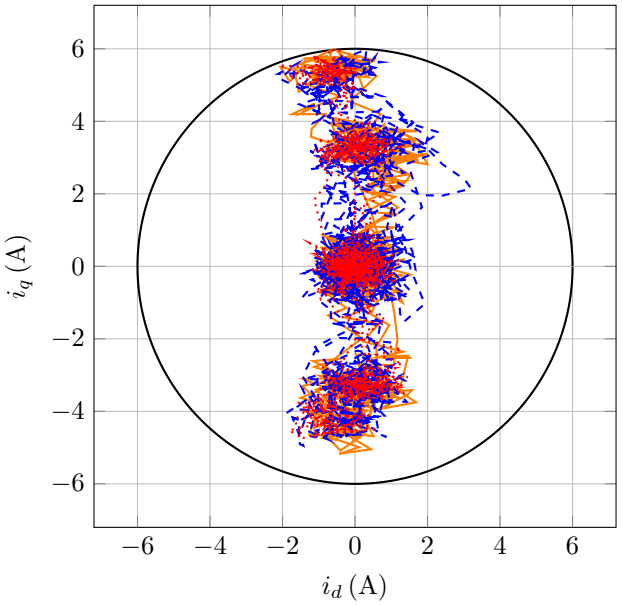

Fig. 5: Current in the *dq*-reference frame during the experiment, red - cCS, blue - rdCS, orange - dtCS.

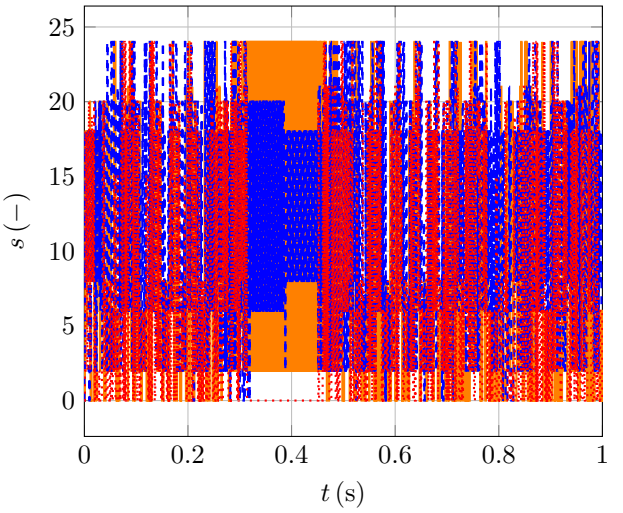

Fig. 6: Applied switching states during the experiment, red - cCS, blue - rdCS, orange - dtCS.

VII. Acknowledgement

The work has been performed in the project A-IQ Ready: Artificial Intelligence using Quantum measured Information for realtime distributed systems at the edge No 101096658/9A22002. The work was co-funded by grants of Ministry of Education, Youth and Sports of the Czech Republic and Chips Joint Undertaking (Chips JU).
The work was supported by the infrastructure of RICAIP that has received funding from the European Union's Horizon 2020 research and innovation programme under grant agreement No 857306 and from Ministry of Education, Youth and Sports under OP RDE grant agreement No CZ.02.1.01/0.0/0.0/17 043/0010085.
The completion of this paper was made possible by the grant No. FEKT-S-23-8451 - "Research on advanced methods and technologies in cybernetics, robotics, artificial intelligence, automation and measurement" financially supported by the Internal science fund of Brno University of Technology.

References

[1] Y.-H. Hwang and J. Lee, "Hev motor comparison of ipmsm with nd sintered magnet and heavy rare-earth free injection magnet in the same size," *IEEE Transactions on Applied Superconductivity*, vol. 28, no. 3, pp. 1–5, 2018.
[2] F. Wang, X. Mei, J. Rodriguez, and R. Kennel, "Model predictive control for electrical drive systems-an overview," *CES Transactions on Electrical Machines and Systems*, vol. 1, no. 3, pp. 219–230, 2017.
[3] P. Karamanakos, E. Liegmann, T. Geyer, and R. Kennel, "Model predictive control of power electronic systems: Methods, results, and challenges," *IEEE Open Journal of Industry Applications*, vol. 1, pp. 95–114, 2020.
[4] X. Sun, M. Wu, G. Lei, Y. Guo, and J. Zhu, "An improved model predictive current control for pmsm drives based on current track circle," *IEEE Transactions on Industrial Electronics*, vol. 68, no. 5, pp. 3782–3793, 2020.
[5] X. Zhang, L. Zhang, and Y. Zhang, "Model predictive current control for pmsm drives with parameter robustness improvement," *IEEE Transactions on Power Electronics*, vol. 34, no. 2, pp. 1645–1657, 2018.
[6] S. G. Petkar, K. Eshwar, and V. K. Thippiripati, "A modified model predictive current control of permanent magnet synchronous motor drive," *IEEE Transactions on Industrial Electronics*, vol. 68, no. 2, pp. 1025–1034, 2021.
[7] W. Xie, X. Wang, F. Wang, W. Xu, R. M. Kennel, D. Gerling, and R. D. Lorenz, "Finite-control-set model predictive torque control with a deadbeat solution for pmsm drives," *IEEE Transactions on Industrial Electronics*, vol. 62, no. 9, pp. 5402–5410, 2015.
[8] Y. Wang, X. Wang, W. Xie, F. Wang, M. Dou, R. M. Kennel, R. D. Lorenz, and D. Gerling, "Deadbeat model-predictive torque control with discrete space-vector modulation for pmsm drives," *IEEE Transactions on Industrial Electronics*, vol. 64, no. 5, pp. 3537–3547, 2017.
[9] Q. Fei, Y. Deng, H. Li, J. Liu, and M. Shao, "Speed ripple minimization of permanent magnet synchronous motor based on model predictive and iterative learning controls," *IEEE Access*, vol. 7, pp. 31791–31800, 2019.
[10] M. Preindl and S. Bolognani, "Model predictive direct speed control with finite control set of pmsm drive systems," *IEEE Transactions on Power Electronics*, vol. 28, no. 2, pp. 1007–1015, 2012.
[11] P. Kakosimos and H. Abu-Rub, "Predictive speed control with short prediction horizon for permanent magnet synchronous motor drives," *IEEE Transactions on Power Electronics*, vol. 33, no. 3, pp. 2740–2750, 2018.
[12] Y. Yu and X. Wang, "Multi-step predictive current control for npc grid-connected inverter," *IEEE Access*, vol. 7, pp. 157756–157765, 2019.
[13] Y. Han, C. Gong, L. Yan, H. Wen, Y. Wang, and K. Shen, "Multiobjective finite control set model predictive control using novel delay compensation technique for pmsm," *IEEE Transactions on Power Electronics*, vol. 35, no. 10, pp. 11193–11204, 2020.
[14] S. Lin, X. Fang, X. Wang, Z. Yang, and F. Lin, "Multiobjective model predictive current control method of permanent magnet synchronous traction motors with multiple current bounds in railway application," *IEEE Transactions on Industrial Electronics*, vol. 69, no. 12, pp. 12348–12357, 2022.
[15] T. Li, X. Sun, G. Lei, Y. Guo, Z. Yang, and J. Zhu, "Finite-control-set model predictive control of permanent magnet synchronous motor drive systems—an overview," *IEEE/CAA Journal of Automatica Sinica*, vol. 9, no. 12, pp. 2087–2105, 2022.
[16] S. P. Boyd and L. Vandenberghe, *Convex optimization*. Cambridge university press, 2004.
[17] S. Ruggieri, "Efficient c4.5 [classification algorithm]," *IEEE Transactions on Knowledge and Data Engineering*, vol. 14, no. 2, pp. 438–444, 2002.